

# Annealing Effect on the Structural and Optical properties of SiO<sub>x</sub> films deposited by HFCVD

Features for its possible use as Optical Sensor

J. A. Luna López  
A. Benítez Lara  
G. García Salgado  
D. Hernández de la Luz  
M. Pacio  
Science Institute-ICUAP-CIDS-BUAP  
Puebla, Pue., 72571, México  
[jose.luna@correo.buap.mx](mailto:jose.luna@correo.buap.mx)

A. Morales Sanchez  
S. A. Perez Garcia  
Centro de Investigación en Materiales Avanzados S. C  
CIMAV-Unidad Monterrey-PIIT  
Apodaca, Nuevo León, México  
[alfredo.morales@cimav.edu.mx](mailto:alfredo.morales@cimav.edu.mx)

**Abstract**— Non-stoichiometric silicon oxide (SiO<sub>x</sub>) with embedded Si nanoparticles (Si-nps) shows novel physical characteristic, which permits its use in optoelectronic devices as photodetectors and light emitters. In this work, a detailed analysis of the structural and optical properties of silicon rich oxide films deposited via hot filament chemical vapor deposition is done. SiO<sub>x</sub> films with different Si content were obtained at different hydrogen flow. FTIR spectra show vibrational bands related to the presence of hydrogen in as-deposited SiO<sub>x</sub> films. This band is more intense as the hydrogen flow is increased, but disappears after thermal annealing. SiO<sub>x</sub> films exhibit a broad photoluminescence (PL) spectra with main peaks at 700 and 750 nm. The PL band at 700 nm is enhanced as the hydrogen content in the SiO<sub>x</sub> films is increased. XPS spectra show a high Si concentration and a low oxygen concentration in the SiO<sub>x</sub> films. Transmittance spectra have a shifted to high wavelength after thermal annealing, and optical band gap was from 2.34 to 3.95 eV.

**Keywords:** SiO<sub>x</sub>; HFCVD; photoluminescence; FTIR; XPS; SEM; UV/Vis spectroscopy.

## I. INTRODUCTION

Non-stoichiometric silicon oxide (SiO<sub>x</sub>,  $x < 2$ ) films have been intensively studied because of their technological importance for silicon-based optoelectronic devices. SiO<sub>x</sub> can be considered as a multi-phase material composed of a mixture of stoichiometric silicon oxide (SiO<sub>2</sub>), not stoichiometric oxide (SiO<sub>x</sub>,  $x < 2$ ) and elemental silicon (as nanoparticles). Si nanoparticles (Si-nps) embedded in a SiO<sub>x</sub> matrix are currently attracting great interest as a candidate for efficient light absorber devices [1-3]. Such devices are highly desirable for the integration of optical signals with electronic data processing circuits in the same chip [4-5]. It has been established that blue and green photoluminescence (PL) observed in SiO<sub>x</sub> films are related by several emitting centers in the silicon oxide, while the nature of the intense PL in orange-red region is still discussed [6-8]. SiO<sub>x</sub> can be prepared by a number of techniques including silicon ion

implantation into the thermal dioxide films [9], reactive sputtering [10-11], co-evaporation [12], low pressure chemical vapor deposition (LPCVD) [13], Hot Filament CVD (HFCVD) [14] and plasma enhanced chemical vapor deposition (PECVD) [15]. In all of these techniques the silicon excess is controlled by changing the process parameters. Thermal treatments are generally used to enhance the luminescent properties of the SiO<sub>x</sub> films.

In this paper, we report on the structural and optical properties (as Si-nanocluster, amorphous silicon, defects, optical band gap energy and PL) of SiO<sub>x</sub> films deposited on silicon substrates with different Si excess. X-ray photoelectron spectroscopy (XPS), Profilometry and Fourier transform Infrared spectroscopy (FTIR) techniques have been used to determine the structure and composition of SiO<sub>x</sub> films. The optical properties were obtained by PL and UV-Vis techniques. The optical band gap of the SiO<sub>x</sub> films; which are widened with respect to the bulk material (c-Si) and also, an intense visible room temperature PL to SiO<sub>x</sub> films is observed. Therefore, the influence of the Hydrogen flow in the Si excess is important, where the optical band gap increased depending of the parameters of deposit. Also, an interesting relationship between the growth temperature; annealing, gas flow, and structural and optical properties can be obtained and analyzed. With this knowledge it is possible to design SiO<sub>x</sub> films with a specific structural and optical characteristic just by a control of the gas flow and growth temperature, these features can be used to optoelectronics devices.

## Experiment

SiO<sub>x</sub> films were deposited on n-type silicon wafers (100) with a resistivity of 1 – 10 Ω-cm and on quartz substrates in a vertical homemade HFCVD reactor. The substrates were cleaned with a metal oxide semiconductor (MOS) standard cleaning process and the native silicon oxide was removed by a HF-Buffer solution. A schematic of the home-made HFCVD configuration is shown in the Fig. 1. HFCVD technique consists in to dissociate molecular hydrogen in atomic

hydrogen using a tungsten filament heated at  $\sim 2000^\circ\text{C}$ . Atomic Hydrogen reacts with the source and it produces the precursors that are transported to the substrate.

SiO<sub>x</sub> films were deposited at three different hydrogen flows 50, 100 and 150 sccm using quartz rods (of 5.3 cm length, 2 mm diameter) like source. The filament-source distance and the distance source-substrate, which determines the growth temperature, were fixed at 3 mm and 5 mm, respectively. After deposition, SiO<sub>x</sub> samples were thermally annealed at 1100 C for 60 minutes in nitrogen atmosphere. Thermally annealed samples are marked as A3-T, B3-T and C3-T for hydrogen flow rates of 50, 100 and 150 sccm, respectively. Table 1 shows the characteristics of the growth films.

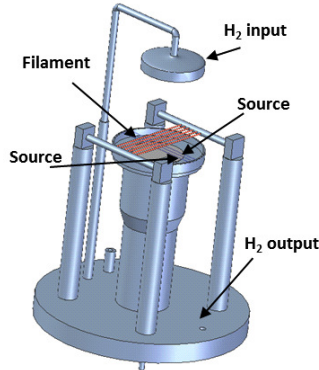


Fig. 1. Homemade HWCVD System.

Fig. 2 shows a scheme of the deposition process.

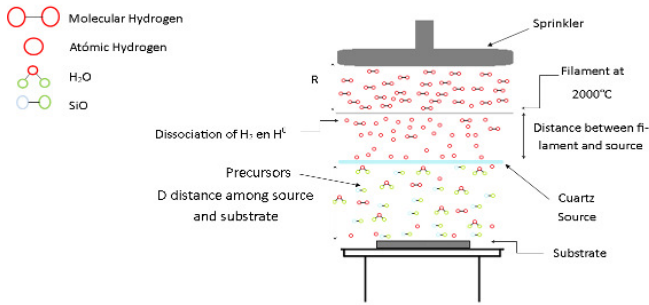


Fig. 2. Schematic of the deposit process.

### I. Characteristics of growth of the SiO<sub>x</sub> films.

Sample	Hydrogen flow (sccm)	Growth Temp (°C)	Annealing (°C)	D <sub>F-S*</sub> (mm)	D <sub>S-S</sub> (mm)	Time (s)
A3	50	890		3	5	5
A3-T	50	890	1100			
B3	100	872				
B3-T	100	872	1100			
C3	150	870				
C3-T	150	870	1100			

\* D<sub>F-S</sub> (Filament-Source), D<sub>S-S</sub> (Source-Substrate).

The compositional and optical properties of the SiO<sub>x</sub> films were obtained using different spectroscopic techniques. FTIR measurements were done using a Bruker system model vector 22. XPS analysis was carried out using an ESCALAB 250Xi Thermo Scientific spectrometer with a monochromatic Al radiation XR15 and energy 20 eV. PL response was measured at room temperature using a Horiba Jobin Yvon spectrometer model FluroMax 3. The samples were excited with a wavelength of 240 nm, and PL response was recorded between 400 and 900nm with 1nm resolution. Transmittance of the SRO films was measured using a UV-vis-NIR Cary 5000 system from Agilent Technologies Inc. The transmittance was collected from 300 to 900 nm with a resolution of 0.5 nm. The thickness of SiO<sub>x</sub> film was measured by a profilometer DEKTAK 150 by Veeco Bruker with a Stylus of 12 μm.

### II. RESULTS

The thicknesses of the SiO<sub>x</sub> films are shown in Fig. 3.

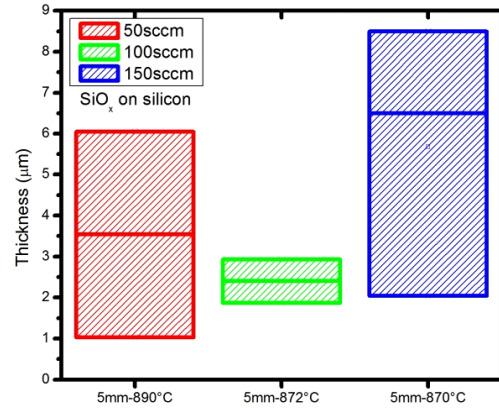


Fig. 3. Thicknesses of the SiO<sub>x</sub> films as a function of the flow ratio.

The FTIR absorption spectra of the SiO<sub>x</sub> films deposited with different Hydrogen flow before and after thermal annealing are shown in Fig. 4. Absorption peaks associated with the stretching ( $1084\text{ cm}^{-1}$ ), bending ( $812\text{ cm}^{-1}$ ) and rocking ( $458\text{ cm}^{-1}$ ) vibration modes of the Si-O-Si bonds in SiO<sub>2</sub> are observed in the SiO<sub>x</sub> films [15-16]. The position of the stretching absorption peak in SiO<sub>x</sub> films show different changes, this peak have a widened peak in the as-growth films, therefore different types of Si-O bonding conformed this stretching peak. The on phase stretching peak position moves toward a higher wavenumber with a larger growth temperature and the out of phase stretching peak position, similarly shows changes with the growth temperature. On the other hand, with annealing all peaks have a similar behaviour as SiO<sub>2</sub> and a shifted toward a higher wavenumber is observed. Table 2 shows only the peak position of the Si-O, Si-Si, Si<sub>2</sub>O<sub>3</sub>, C-O, Si-C and Si-H bonds to 50, 100 and 150 of gas flow.

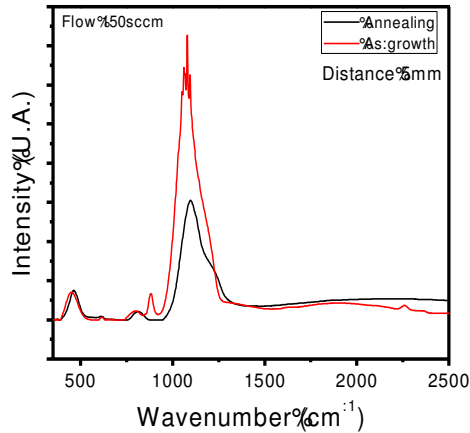
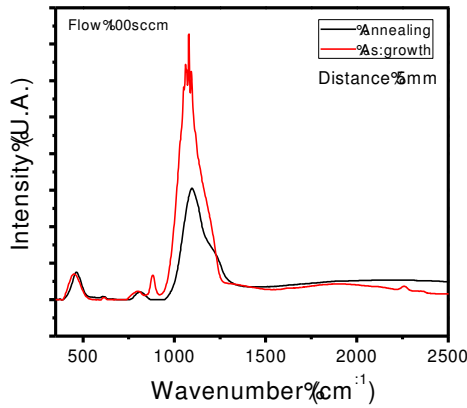
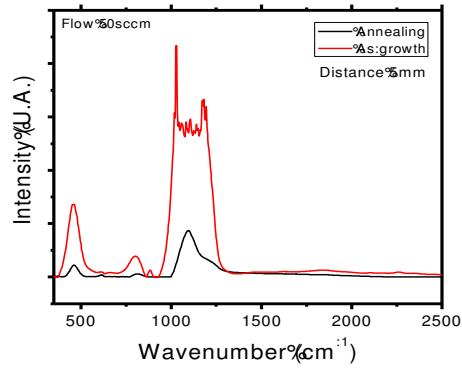


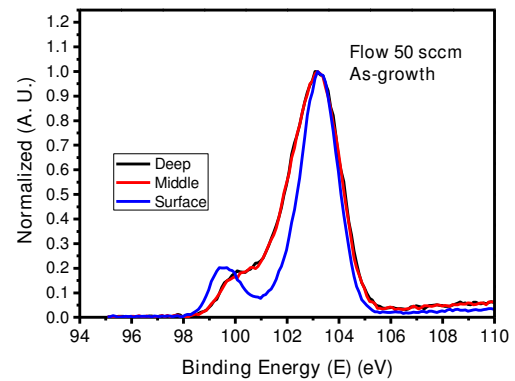
Fig. 4. Absorption spectra of the SiOx films as growth and with annealing for different growth temperatures and flow rates, a) flow 50 sccm, b) flow 100 sccm and c) 150 sccm.

Fig. 5 shows XPS-Si 2p spectra and its evolution in the surface, volume (middle) and SiOx/Si interface (deep) of different SiOx films.

TABLE II. PEAKS POSITION OF THE FTIR SPECTRA OF THE SiOx FILMS TO DIFFERENTS FLOW RATIOS.

Vibrational Peaks	Samples As-growth and Annealing						
	Flow	50sccm		100sccm		150sccm	
	SiO <sub>2</sub>	A3	A'3	B3	B'3	C3	C'3
Si-O rocking	458	460	460	453	463	457	469
Si-Si	--	613	611	619	609	611	609
Si <sub>k</sub> -H	--	657	--	663	--	673	--
Si-O bending	812	800	819	798	812	800	810
Si-H δ Si <sub>2</sub> O <sub>3</sub>	--	885	--	881	--	881	--
Si-O stretching on phase	1082	1024	1095	1008	1097	1020	1091
Si-O stretching out of phase	1177	1187	1172	1137	1166	1170	1101
C-O bending	--	1847	1874	1921	1863	--	1629
Si-H stretching	--	2262	--	2258	--	2258	--
Si-C stretching	--	2362	2356	2360	2360	2362	--

The Si 2p binding energies are normally about 99-103 eV. It is widely accepted that the Si 2p photoelectron peak of SiOx contains five components, corresponding to a non-oxidized state and four different oxidation states of Si [17-18]. The four oxidation states, as well as the unoxidized state, can be modeled as tetrahedral bonding units, in which a central Si atom is bonded to (4-n) Si atoms and n oxygen atoms (Si-Si<sub>4-n</sub>O<sub>n</sub>) with n = 0 to 4. The variation of the oxidation states of the SiOx films lead to peak position's shift, as shown in Figure 5. Two main peaks at about 99 eV and 103 eV are present and they are attributed to Si and SiO<sub>2</sub>, respectively, and any variation could be attributed to sub oxidized silicon [19-20]. The increasing electro-negativity of the Si-O bond relative to the Si-Si bond results in a shift to a higher binding energy of the core level electrons in the silicon.



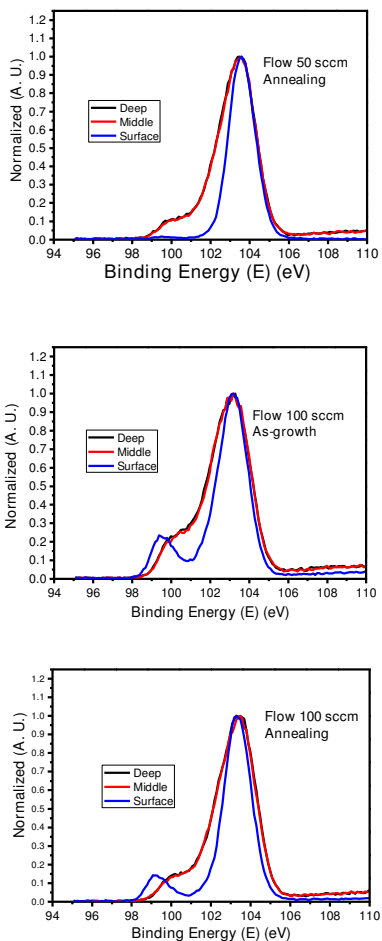


Fig. 5. Si 2p XPS spectra of the SiOx films deposited at different hydrogen flow before and after thermal annealing.

Fig. 6 shows the XPS deep profile composition of different SiOx with different Hydrogen flow. The composition of SiOx is shown in Table III.

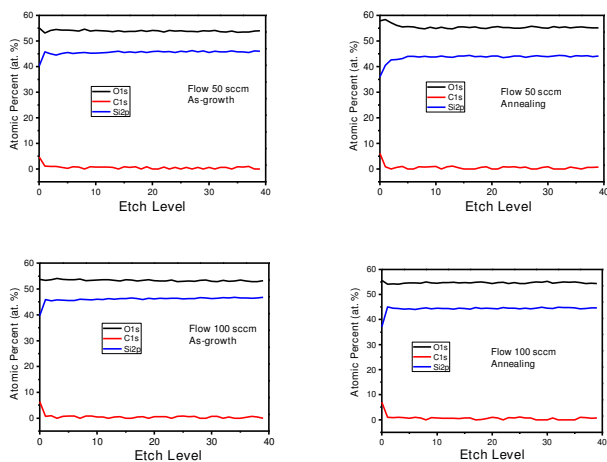


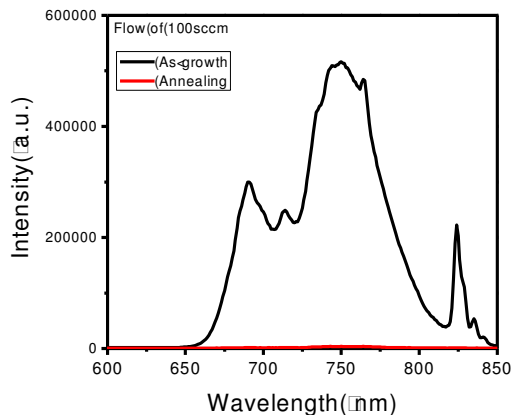
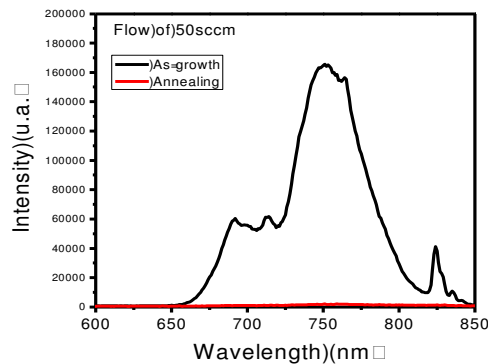
Fig. 6. XPS spectra show the composition of the SiOx films.

TABLE III. COMPOSITIONAL RESULTS (ATOMIC PERCENTAGES OF OXYGEN (O), C AND SILICON (SI)) OF THE SiOx FILMS OBTAINED BY XPS.

Samples	Surface			Middle			Deep		
	Si	O <sub>2</sub>	C	Si	O <sub>2</sub>	C	Si	O <sub>2</sub>	C
A3	40.14	55.07	4.78	45.43	53.73	0.83	46.014	53.98	0
A3-T	36.4	57.81	6.18	43.74	54.90	0.60	44.10	55.06	0.82
B3	39.75	53.77	6.46	46.39	53.60	0.63	46.80	53.19	0
B3-T	37.14	55.62	6.93	44.53	54.77	0.06	44.68	54.31	0.68

Figure 7 shows the PL spectra from SiOx films for the three different hydrogen flows. A wide PL spectrum is observed for all the as-growth samples. Two main peaks are placed around 690 and 750 nm and their intensity depends on the hydrogen flow. The PL peak placed at 700 nm is more intense as the hydrogen flow is increased. The PL quenches after the SiOx films are thermally annealed, at the same time that the presence of hydrogen disappears.

The Transmittance spectra display a wavelength shift of the absorption edge from 550 to 350nm to sample A3 and A3-T, respectively, as is shown in the Fig. 8. The transmittance of all films is among 70% to 80% from 500nm to 900nm and reduces to zero for wavelengths below 500 nm at 50sccm, 350nm at 100 and 150sccm. It implies a change in the optical band gap of the material, as it is shown in the Table IV. The optical band gap was obtained by Tauc plot method [20-21]; the results are illustrated in the table IV and Figure 9 shows an example.



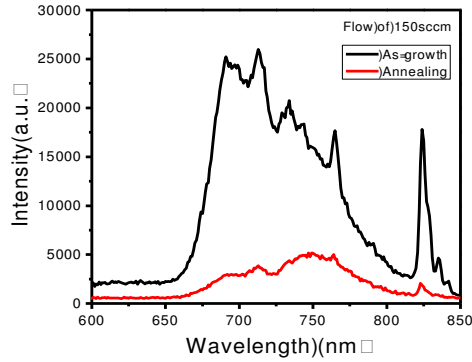


Fig. 7. PL spectra of SRO films, 50sccm, 100sccm and 150sccm.

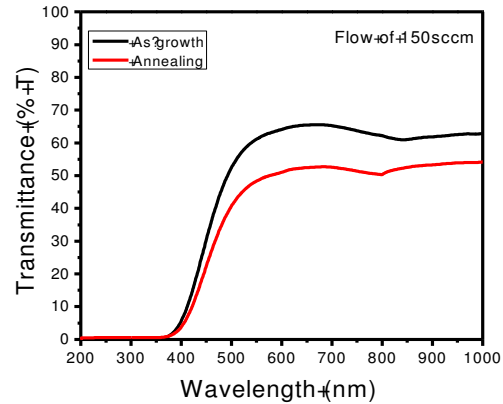
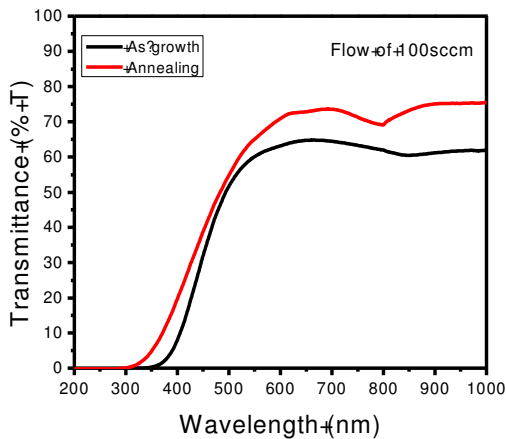
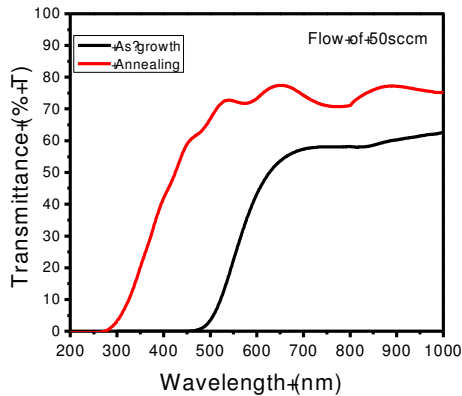


Fig. 8. UV-Vis transmittance spectra for the three flows, 50sccm, 100sccm and 150sccm.

### III. DISCUSSION

The shape of the stretching peak in FTIR spectra let us differentiate between SiO<sub>x</sub> films as-growth and annealing. The stretching peak in SiO<sub>x</sub> films as-growth is continuous and wide. However, with annealing the films show a thin stretching peak in FTIR spectra. The thin stretching peak means that the film is not amorphous and the shape of the peak looks like SiO<sub>2</sub> stretching. In general, the stretching peak is defined by the hydrogen flow and the growth temperature. In case of 50 sccm, all the FTIR spectra of the SiO<sub>x</sub> films show that the stretching peaks have additional peaks with shape different to typical stretching Si. Diverse silicon-oxygen, silicon-hydrogen bonds and amorphous silicon form these SiO<sub>x</sub> films. In the FTIR spectra of the SiO<sub>x</sub> films are observed typical stretching peaks (as SiO<sub>2</sub>) obtained at a hydrogen flow of 100 sccm as is show in the Fig. 4. The Si-Si bond appears near at 611 cm<sup>-1</sup>. Also, the increment of the intensity of H-Si bonds (663, 880 and 2250 cm<sup>-1</sup>) changed by the decrement of the temperature, it occurs during the deposition, which at the same time occurs an annealing and it forces the hydrogen (H) desorption. It was shown in previously works [14, 21].

The PL intensity of the SRO films is weak at higher temperatures. SiO<sub>x</sub> films growing to a hydrogen flow of 100 sccm and 5 mm of substrate-source distance showed the higher PL intensity. The decrement of the PL intensity at higher temperature is by desorption of H<sub>2</sub>, as it was shown by FTIR, where the highest deposition temperature the peak of Si-H at 870cm<sup>-1</sup> is reduced with respect to the others temperatures deposition. Desorption of H<sub>2</sub> increments the presence of nonradiative centers. The deposit at 100sccm hydrogen flow with a substrate-source distance of 5 mm was showed a good homogeneity and highest intensity of PL. Our supposition about the homogeneity is that the deposition temperature is constant over the substrate. On the other hand, the optical band gap is bigger to the sample deposit at 100sccm hydrogen flow and in all case the optical band gap increase with annealing.



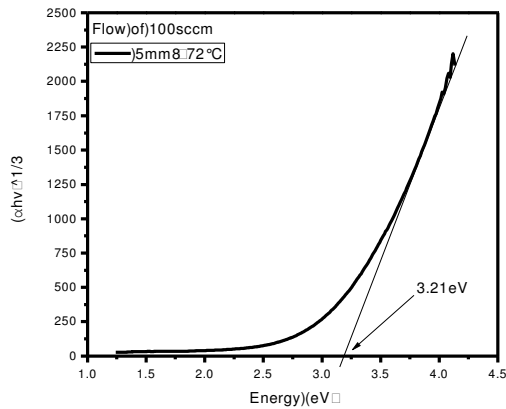


Fig. 9. Tauc's Method to calculate bandgap.

TABLE V. OPTICAL BAND GAP OF THE SRO FILMS.

Source-substrate distance (mm)	Bandgap at 50sccm (eV)		Bandgap at 100sccm (eV)		Bandgap at 150sccm (eV)	
	As-growth	Annealing	As-growth	Annealing	As-growth	Annealing
5	2.34	4.33	3.21	3.95	2.7	2.95

#### IV. CONCLUSION

The properties of the films SiOx deposited by HFCVD presents different changes due to the growth temperature and the flows rate. The flows have high influence in the growth temperature. The deposit temperatures with a flow of 50sccm have a behavior different with respect other as-growth films mainly in the stretching peak, as it was observed by FTIR that shows the different types bond. In this case, the precursors remain more time on the substrate surface, but with annealing, a separation of phase is present. Desorption of Hydrogen was observed to highest temperatures with the annealing, and it has an effect strong in the PL. The PL tendency in each flow rate is that there is a temperature and flow with the better intensity PL. Therefore, the flow of hydrogen has influence strong in the PL. Films can be obtained by HFCVD with different characteristics structural and optical. The conditions to obtain SiOx films were developed in this study and these films showed very good absorption and emission of light.

#### ACKNOWLEDGMENT

This work has been partially supported by CONACyT-154725 and VIEP-BUAP-2014. The authors acknowledge

INAOE, IFUAP and CIMAV-Monterrey laboratory for their help in the samples measurements.

#### REFERENCES

- [1] Nayfeh, M.; Rao, S.; Barry, N.; Therrien, J.; Belomoin, G.; Smith, A.; Chaieb, S., 2002, Appl. Phys. Lett., 79, 1249-1251.
- [2] Pavesi, L.; Dal Negro, L.; Mazzoleni, C.; Franzo, G.; Priolo, F. 2000, Nature, 480, 440-444.
- [3] Luterova, K.; Pelant, I.; Mikulskas, I.; Tomasiunas, R.; Mueller, D.; Grob, J.-J.; Rehspringer, J.-L.; Honerlage, B. 2002, J. Appl. Phys., 91, 2896-2900.
- [4] Sui, G.G.; Wu, X.L.; Gu, Y.; Boa, X.M. Appl. Phys. Lett. 1999, 74, 1812-1814.
- [5] Tamura, H.; Ruckschloss, M.; Wirschem, T.; Veprek, S. Appl. Phys. Lett. 1994, 65, 1537-1539.
- [6] Kenyon, A.J.; Trwoga, P.F.; Pitt, C.W.; Rehm, G. J. Appl. Phys. 1996, 79, 9291-9300.
- [7] Lin, G. R.; Lin, C. J.; Lin, C. K.; Chou, L. J.; Chueh, Y.-L. J. Appl. Phys. 2005, 97, 094306
- [8] Chen, X.Y.; Lu, Y.F.; Wu, Y.H.; Cho, B.J.; Liu, M.H.; Dai, D.Y.; Song, W.D. J. Appl. Phys. 2003, 93, 6311-6319.
- [9] L. Pavesi, L. Dal Negro, L. Mazzoleni, G. Franzo, and F. Priolo, Nature, vol.408, pp440, 2000.
- [10] O. Hanaizumi, K. Ono, and Y. Ogawa, Appl. Phys. Lett, vol.82, pp.538-540, 2003.
- [11] Kohno, K.; Osaka, Y.; Toyomura, F.; Katayama, H. Jpn. J. Appl. Phys. 1994, 33, 6616-6622.
- [12] Y. C. Fang, W. Q. Li, L. J. Qi, L. Y. Li, Y. Y. Zhao, Z. J. Zhang, and M. Lu, Nanotechnology, vol.15, pp.495-500, 2004.
- [13] D.Dong et al, J.Electrochem. Soc., vol.125, pp.819-823, 1978.
- [14] J. A. L. López, G. G. Salgado, A. P. Pedraza, D. E. V. Valerdi, J. C. López, A. M. Sánchez, T. D. Becerril, E. R. Andrés, and H. J. Santiesteban, Structural and Optical Properties of SiOx Films Deposited by HFCVD, Procedia Engineering, vol. 25, no. 2010, pp. 304–308, Jan. 2011.
- [15] P. G. Pai, S. S. Chao, Y. Takagi, and G. Lucovsky, J. Vac. Sci. Technol. A, 4(3) (1986) 689-694.
- [16] Pereyra, Alayo, Thin solid Films, 402 (2002) 154-161
- [17] Shinji Hayashi, Shinichi Tanimoto, and Keiichi Yamamoto: Analysis of surface oxides of gasevaporated Si small particles with infrared spectroscopy, high resolution electron microscopy, and xray photoemission spectroscopy. J Appl Phys 1990, 68(10): 5300.
- [18] L.B. Ma, A. L. Ji, C. Liu, Y. Q. Wang, and Z. X. Cao: Low temperature growth of amorphous Si nanoparticles in oxide matrix for efficient visible photoluminescence. J Vac Sci Technol B 2004, 22: 2654
- [19] F. Iacona, G. Franzo, and C. Spinella: Correlation between luminescence and structural properties of Si nanocrystals. J Appl Phys 2000, 87(3): 1295.
- [20] F. Iacona, C. Borgiono, and C. Spinella: Formation and evolution of luminescent Si nanoclusters produced by thermal annealing of SiOx films. J Appl Phys 2004, 95(7): 3723.
- [21] J.A.Luna López, J.C. López, D.E.V. Valerdi, G.G. Salgado, T. Díaz-Becerril, a P. Pedraza, and F.J.F. Gracia, Nanoscale Res. Lett. 7, 604 (2012).
- [22] Pankove JI: Optical Processes in Semiconductors. Englewood Cliffs, New Jersey: Prentice Hall; 1971.

